Research Article | Vol. 1, No. 4 / 15 December 2018 / OSA Continuum 1304

Carrier-envelope phase sensitive inversion driven by few-cycle pulse pairs

BING ZENG AND LINGZE DUAN*

Department of Physics, the University of Alabama in Huntsville, Huntsville, AL 35899, USA
*ld0003@uah.edu

Abstract: The response of a two-level system to a few-cycle pulse pair has been investigated with a special focus on the relation between population inversion and the carrier-envelope phases (CEPs) of the two pulses. The goal is to explore possible schemes of coherent control based on sequential ultrafast pulses. Simulation results indicate a close CEP-inversion relation, which stems from the coherent nature of the interaction. The impact of the pulse amplitudes is evaluated and is shown to create weak-field and strong-field interaction regions with drastically different characteristics. The important role of carrier-wave Rabi flopping in defining these characteristics is also analyzed. Finally, advantages of the method and experimental realization are discussed.

1. Introduction

Coherent control with sequential optical pulses or pulse trains has attracted a lot of interest in recent years because of its unique capability in achieving coherent population transfer among quantum states [1–7]. Within this context, schemes such as adiabatic passage [2–5], coherent accumulation [6,7], and coherent population oscillation [8] have been investigated. Earlier studies on pulse trains interacting with atomic systems focus exclusively on pulses with durations much longer than the optical cycles [9–12]. With recent advance in femtosecond lasers, ultrafast pulses containing only few optical cycles have become experimentally attainable [13]. This triggers growing interest in understanding the interactions between atomic systems and few-cycle pulse (FCP) sequences [3,8,14].

From a theoretical point of view, several unique aspects arise when pulse width enters the few-cycle regime. Strong field typically has to be assumed [15] and the slowly-varying-envelope approximation (SVEA) is no longer valid [16,17]. The near-resonance approximation also becomes invalid in general because of the ultra-broad pulse spectrum as well as the possible large detuning between carrier frequencies and atomic transition frequencies. These new features lead to the breakdown of the rotating-wave approximation (RWA) and the concept of pulse area [18–20], which form the foundation of the widely accepted optical Bloch equations [21]. As a result, theoretical models for atom-field interactions in the few-cycle regime are generally more complicated and solving these problems usually involve numerical simulations, although some success has been achieved in finding analytical solutions under specific conditions (e.g., far-off-resonant excitation [22,23]).

One important concept associated with FCP is carrier-envelope phase (CEP), which is defined as the phase of carrier field relative to the peak of pulse envelope. When pulse width is comparable to the carrier cycle, the impact of CEP on the exact pattern of electromagnetic field within the pulse becomes much more significant [24]. Over the last decade, the effect of CEP in coherent control of atomic systems has been the topic of several reports [25–29]. Notably, Mücke *et al.* studied the role of CEP in carrier-wave Rabi flopping [25]; Jirauschek *et al.* reported CEP-sensitive inversion in two-level atomic systems [26]; Wu and Yang showed the profound effects of CEP on atomic coherence and quantum beats [27]; Yang *et al.* investigated CEP-dependent coherence in an artificial atomic system made of semiconductor quantum wells [28]; and more recently, Li *et al.* successfully probed and modeled CEP-dependent interference

#338421 https://doi.org/10.1364/OSAC.1.001304
Journal © 2018 Received 10 Jul 2018; revised 12 Nov 2018; accepted 14 Nov 2018; published 10 Dec 2018

OSA CONTINUUM

between one-photon and multi-photon transitions excited by few-cycle radio-frequency pulses [29]. All these prior efforts, however, dealt with individual FCP. To the best of our knowledge, the impact of CEP on coherent control has not been explicitly studied in the context of sequential pulses. Yet, light-matter interactions under FCP sequences are fundamentally significant because their ramifications strongly depend on the coherence properties of the atomic system in a highly nonlinear fashion, which is generally not revealed in the interactions with single pulses.

In the current paper, we numerically investigate the response of a two-level system (TLS) to a FCP pair, with a special emphasis on the relations between population inversion and various parameters of the two pulses. We also seek to identify the role pulse amplitudes play in such a relation and explore the physical picture underlying the simulation results. Finally, we attempt to put our results into experimental contexts and discuss the potential of using FCP pairs as a practical scheme for coherent control. The paper is organized as follows: Section II outlines the theoretical model, Section III reports the numerical results, and Section IV presents discussions and conclusions.

2. Theoretical model

Our analysis considers two consecutive FCPs interacting with a TLS medium. The medium is treated as optically thin so that propagation effects can be neglected. This allows the Maxwell-Bloch equations to be simplified to the Bloch equations. For the current work, we choose the general form of the Bloch equations within the dipole approximation but without invoking the RWA [8]. For a TLS defined by a transition frequency ω_{ba} and a Bloch vector (u, v, w), the Bloch equations can be written as:

$$\dot{u} = \omega_{ba} v - \frac{u}{T_2}, \tag{1a}$$

$$\dot{v} = -\omega_{ba} u - 2\Omega_R(t) w - \frac{v}{T_2}, \tag{1b}$$

$$\dot{w} = 2\Omega_R(t) v - \frac{w+1}{T_1}, \tag{1c}$$

where the overdot denotes time derivative. T_1 and T_2 are spontaneous decay time and dipole dephasing time, respectively. $\Omega_R(t) = \mu E(t)/\hbar$ is instantaneous Rabi frequency, with E(t) representing the driving field and μ representing the transition dipole moment. Note that the factor 2 in front of $\Omega_R(t)$ is due to the assumption of a $\Delta m = 0$ transition [30]. Since the focus of our analysis is on the coherent dynamics of the TLS and the pulse durations and the relative pulse delay used in the simulations are smaller than the typical values of T_1 and T_2, the terms associated with T_1 and T_2 are neglected in the current study.

The driving field consists of two transform-limited (no chirp) Gaussian pulses separated by a time delay. The corresponding time-dependent Rabi frequency is given by

$$\begin{aligned} \Omega_R(t) = {} & \Omega_{01} \exp[-(t/\tau)^2] \cos(\omega_c t + \varphi_{CE1}) \\ & + \Omega_{02} \exp\{-[(t-\Delta t)/\tau]^2\} \cos[\omega_c (t-\Delta t) + \varphi_{CE2}] \end{aligned}, \tag{2}$$

where ω_c is the carrier frequency and τ represents the pulse width. Ω_{01} and Ω_{02} are the peak Rabi frequencies of the leading and the trailing pulses, respectively. φ_{CE1} and φ_{CE2} are the CEPs of the two pulses. Δt is the relative pulse delay.

In order to put our numerical results into a context, we follow a similar treatment by Mücke *et al.* [14] and choose the transition energy between the two levels to be 1.424 eV (coinciding with the GaAs band gap) and a typical value of the transition dipole moment to be $\mu = 0.5e$ nm. Throughout the work, we assume the two pulses have the same full-width-at-half-maximum (FWHM) duration of 5 fs. The carrier wavelength is set to be 800 nm (the typical wavelength

OSA CONTINUUM

of Ti:Sapphire lasers), which leads to a carrier frequency detuning of $\Delta = \omega_c - \omega_{ba} = 0.089\omega_{ba}$. The initial values of the Bloch vector are (0, 0, -1) for all the simulations while five parameters are considered adjustable: the peak Rabi frequencies of the two pulses, the CEPs of the two pulses, and relative pulse delay. The standard fourth-order Runge-Kutta method is used to solve Eq. (1a)–(1c).

3. Numerical results

3.1. Effects of the trailing pulse

First, we investigate the impact of the trailing pulse on the inversion of the TLS. The questions we seek to answer here are: Given a known initial state, which is defined by fixing the parameters of the leading pulse as well as the relative pulse delay, what is the relation between φ_{CE2} and the final inversion w_f and how does Ω_{02} affect this relation? The leading pulse is chosen in such a way that it drives the inversion from $w = -1$ to $w = 0$. The relative pulse delay is set at 50 fs. This choice of initial state, although somewhat arbitrary, does not qualitatively impact the results to be discussed. Ω_{02} is varied within the range of 0 to 3.2 ω_c, and in each case, φ_{CE2} is adjusted between $-\pi$ and $+\pi$.

The time-evolutions of the inversion under several values of φ_{CE2} are summarized in Fig. 1(a). The peak Rabi frequency of the trailing pulse is fixed at $\Omega_{02} = 0.833\omega_c$ in this case. The trailing pulse induces a transient process in which the inversion oscillates. The final inversion level upon the passage of the trailing pulse exhibits a clear dependence on φ_{CE2}. The exact form of this dependence is revealed by plotting w_f directly against φ_{CE2}, which is shown in Fig. 1(b) for several values of Ω_{02}. When Ω_{02} is below a certain level, the relation between w_f and φ_{CE2} is found to be very close to a sinusoidal relation, with the corresponding "amplitude" and "phase" varying with Ω_{02}. When Ω_{02} is high enough, however, the inversion-phase dependence begins to deviate from a simple oscillation (blue dash-dotted trace in Fig. 1(b)), suggesting the onset of a strong nonlinear interaction between the pulse and the TLS. Our simulation indicates that this change of behavior occurs when Ω_{02} reaches about $1.57\omega_c$.

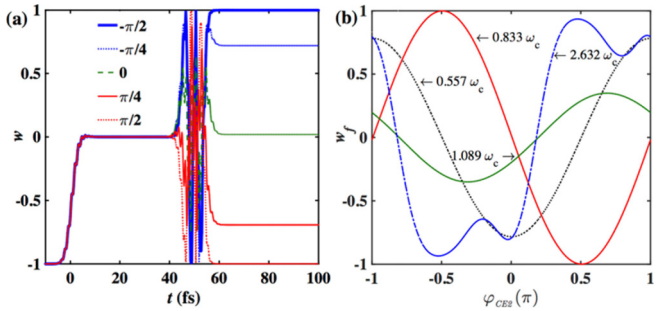

Fig. 1. (a) Inversion evolution in the simulated TLS due to a pair of 5-fs pulses. The leading pulse (at $t = 0$) drives the inversion from $w = -1$ to $w = 0$. The trailing pulse (delayed by 50 fs), with an amplitude equivalent to a peak Rabi frequency of $0.833\omega_c$ and a CEP varying between $-\pi/2$ and $+\pi/2$, generates a final inversion level that clearly depends on the CEP. (b) The final inversion w_f versus the CEP of the trailing pulse φ_{CE2} for several values of peak Rabi frequency Ω_{02}.

3.2. Strong field vs. weak field

To investigate the inherent impact of Rabi oscillation on the CEP-sensitive inversion, we vary the peak Rabi frequency Ω_{02} while keeping φ_{CE2} fixed at certain values. Figure 2(a) shows w_f as a function of Ω_{02} at three different choices of φ_{CE2}. Once again, the relation between w_f and Ω_{02}

OSA CONTINUUM

appears to be oscillatory and quasi-periodic until Ω_{02} reaches approximately $1.57\omega_c$, at which point the behavior of the inversion becomes highly irregular. This characteristic change suggests that the atom-field interaction enters a highly nonlinear regime. To understand the underlying physics, we notice that Ω_{02} corresponds to the absolute maximum value of the instantaneous Rabi frequency the trailing pulse can possibly generate. However, for gauging the overall impact of the pulse, it is reasonable to use a somewhat "averaged" field instead of the absolute peak field. One plausible strategy is to average a sinusoidally oscillating field over a half cycle. If we define an average field based on the center half cycle of a cosine pulse, the corresponding average Rabi frequency is related to Ω_{02} through the simple relation $\Omega_{Ra2} = (2/\pi)\,\Omega_{02}$. In the case of $\Omega_{02} = 1.57\omega_c$, the average Rabi frequency is approximately equal to the carrier frequency: $\Omega_{Ra2} \approx \omega_c$. It is therefore clear that the irregular behavior of w_f under strong field is due to carrier-wave Rabi flopping, which occurs when Rabi frequency becomes comparable to the carrier frequency [14].

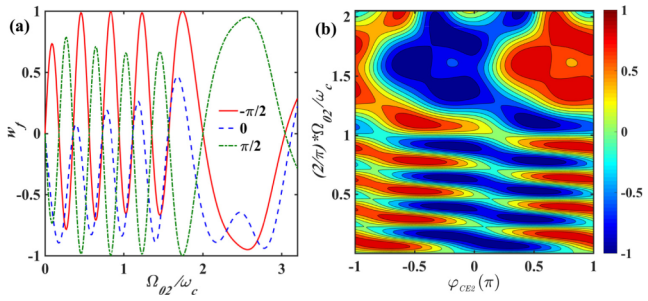

Fig. 2. (a) The final inversion w_f versus the peak Rabi frequency of the trailing pulse Ω_{02} with φ_{CE2} equal to -π/2, 0 and +π/2. (b) A contour plot of w_f as a function of both φ_{CE2} and the average Rabi frequency Ω_{Ra2} (expressed in terms of Ω_{02} and ω_c).

The overall dependence of the final inversion on both the average Rabi frequency and the CEP of the trailing pulse can be revealed by mapping w_f on a two-dimensional space formed by φ_{CE2} and Ω_{Ra2} in a contour plot. This is shown in Fig. 2(b). Two distinctive regions can be identified on the plot. When the average Rabi frequency is below the carrier frequency, w_f follows a regular, periodic relation over φ_{CE2}. This can be viewed as a "weak-field" region. As the average Rabi frequency grows past ω_c, however, the regular pattern gradually gives way to an irregular, patchy pattern, indicating the dominance of strong nonlinear interactions. This can be defined as a "strong-field" region. The two regions are separated by the $\Omega_{Ra2} = \omega_c$ condition, demonstrating the critical role of carrier-wave Rabi flopping in determining the characteristics of atom-field interactions.

3.3. *Effects of the leading pulse*

The impact of the leading pulse on the final inversion w_f is studied following a similar approach as the analysis of the trailing pulse. In this case, Ω_{02} and φ_{CE2} are fixed and so is the relative pulse delay Δt. Ω_{01} and φ_{CE1} are adjusted and the corresponding levels of w_f are computed. Figure 3 summarizes key results of the analysis, where $\Omega_{02} = 0.117\omega_c$ and $\varphi_{CE2} = -0.779\pi$ are used. Qualitatively, w_f exhibits a similar dependence on φ_{CE1} as it does on φ_{CE2}. This similarity is clearly evident when comparing Fig. 3(a) with Fig. 1(b). Furthermore, the CEP sensitivity of w_f is modulated by Ω_{01} in a similar fashion as it is modulated by Ω_{02}. A regular, periodic dependence over φ_{CE1} is featured in the weak-field region, which is in contrast to a highly irregular relation in the strong-field region, as shown in Fig. 3(b). The two regions are separated by the leading-pulse version of carrier-wave Rabi flopping, i.e. $\Omega_{Ra1} = (2/\pi)\,\Omega_{01} = \omega_c$.

The similarity between the leading pulse and the trailing pulse in their effects on w_f highlights the coherent nature of the current scheme. Here, the leading pulse serves as a "stimulator" to

OSA CONTINUUM

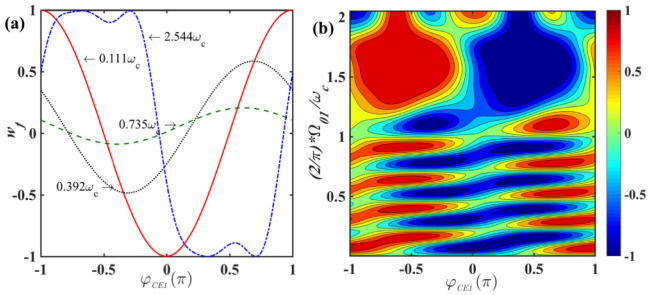

Fig. 3. (a) The final inversion w_f versus the CEP of the leading pulse φ_{CE1} for several values of peak Rabi frequency Ω_{01}. (b) A contour plot of w_f as a function of both φ_{CE1} and the average Rabi frequency Ω_{Ra1} (expressed in terms of Ω_{01} and ω_c).

excite atomic coherence in the TLS. The TLS in turn becomes a "messenger" to transfer phase coherence from the leading pulse to the trailing pulse. Through this process, the population inversion of the TLS is modulated by the CEPs of both pulses. Such a coherence-transfer process is clearly revealed by examining the impact of relative pulse delay Δt on CEP-sensitive inversion. Figure 4(a) shows w_f plotted as a function of both Δt and φ_{CE2}. The results are obtained with the same combination of Ω_{01}, φ_{CE1}, and Ω_{02} as in Fig. 1(a), with Ω_{01} and Ω_{02} both in the weak-field region. The apparent periodicity along the axis of Δt suggests that the dipole moment of the TLS oscillates at an intrinsic frequency in the absence of external excitation. This intrinsic cycle is found to be 2.904 fs based on the period shown in Fig. 4(a). The corresponding frequency of 344.3 THz exactly matches the transition frequency ω_{ba} used in the simulation. The physical picture of this coherent oscillation is easy to understand by inspecting the Bloch equations. In the absence of external field and relaxations, the general solution for the Bloch equations is $(sin\,\omega_{ba}t, cos\,\omega_{ba}t, w_0)$, where w_0 is a constant defined by the initial condition. In our case, w_0 is the inversion caused by the leading pulse, which is chosen to be zero (see Fig. 1(a)). This corresponds to the scenario where the Bloch vector rotates along the equator of the Bloch sphere at a rate equal to ω_{ba}. When the trailing pulse arrives, its electromagnetic field interacts with the TLS in a manner similar to interference between two oscillatory signals, with both the CEP of the pulse and the phase of the Bloch vector directly dictating the outcome of the interaction. This is evident from the straight-line pattern displayed in Fig. 4(a), which, in essence, is a map of

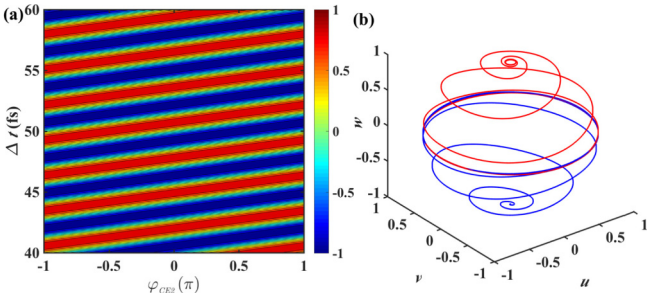

Fig. 4. (a) The final inversion w_f as a function of both φ_{CE2} and the relative pulse delay Δt. The periodic straight diagonal pattern indicates coherent beating between the pulse and the atomic dipole moment. $\Omega_{02} = 0.833\omega_c$ is assumed in this case. (b) Bloch vector trajectories under the excitation of the leading pulse (blue) and the trailing pulse (red). The inversion is driven from $w = -1$ to $w = 0$ by the leading pulse and then from $w = 0$ to $w = +1$ by the trailing pulse.

OSA CONTINUUM

equal-phase lines. A numerical demonstration of the entire process is shown in Fig. 4(b), where the Bloch vector migrates from the $w = -1$ pole to the equator under the excitation of the leading pulse (blue) and, after a brief delay, continues to travel upward until finishing at the $w = +1$ pole under the action of the trailing pulse (red).

3.4. CEP dependence of the final inversion

Finally, we investigate how the final inversion depends on the CEPs of both pulses. Here, we fix Ω_{01}, Ω_{02} and Δt while leaving φ_{CE1} and φ_{CE2} as adjustable parameters in the calculation of w_f. The scheme is further divided into four scenarios based on the relative scales of Ω_{01} and Ω_{02}, and the results are summarized in Fig. 5. Figure 5(a) shows the dependence of w_f on φ_{CE1} and φ_{CE2} when both Ω_{01} and Ω_{02} are in the weak-field region. The straight diagonal pattern suggests that the final inversion is determined by the CEP difference between the two pulses, i.e. $\varphi_{CE2} - \varphi_{CE1}$, in this scenario. This result is in agreement with the physical picture of coherence transfer by the TLS. Figure 5(b) and (c) correspond to the cases where one of the peak amplitudes (Ω_{02} for Fig. 5(b) and Ω_{01} for Fig. 5(c)) is in the strong-field region. Under such conditions, the diagonal contour lines are distorted so the simple dependence of w_f on $\varphi_{CE2} - \varphi_{CE1}$ no longer holds true. But the distortion nevertheless only occurs along one dimension. Figure 5(d) shows the scenario with both Ω_{01} and Ω_{02} in the strong-field region. Distortions of the contour lines can be seen along both dimensions and the overall pattern becomes more irregular.

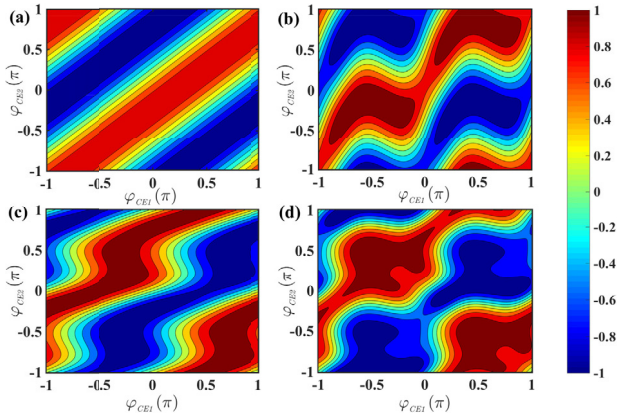

Fig. 5. The final inversion w_f as a function of both φ_{CE1} and φ_{CE2} with various scale combinations of Ω_{01} and Ω_{02}: (a) $\Omega_{01} = 0.111\omega_c$, $\Omega_{02} = 0.117\omega_c$. (b) $\Omega_{01} = 0.111\omega_c$, $\Omega_{02} = 2.443\omega_c$. (c) $\Omega_{01} = 2.708\omega_c$, $\Omega_{02} = 0.231\omega_c$. (d) $\Omega_{01} = 2.708\omega_c$, $\Omega_{02} = 2.378\omega_c$.

4. Discussions and conclusion

The result shown in Fig. 5 highlights some of the key advantages of coherent inversion control using FCP pairs. Compared to schemes based on a single FCP, which often require the peak Rabi frequency of the pulse be comparable to the carrier frequency in order to produce appreciable effects [23,26], the pulse-pair scheme best operates in the weak-field region, where the peak Rabi frequencies of both pulses can be at least one order of magnitude lower without compromising phase sensitivity (see Fig. 5(a) caption). This means the peak power requirement can be reduced by at least two orders of magnitude, making the scheme much easier to realize experimentally. The underlying physics for this lower power requirement is the excitation of atomic coherence in the TLS by the leading pulse. The dipole moment oscillation leads to an atom-field interaction (with the trailing pulse) much like interference between two oscillatory signals, where the outcome is highly sensitive to the phases of the oscillations. Moreover, as shown in Fig. 5(a), the final

OSA CONTINUUM

inversion only depends on the CEP difference between the two pulses once the pulse amplitudes are fixed (under weak-field conditions). This eliminates the needs for CEP control of individual pulses, which significantly simplifies the experimental system.

Of course, when the current scheme is brought into the broader context of coherent quantum state control, it is inevitable to draw comparison between this method and the standard approach based on pulse area [21]. A natural question to ask at this point is: Beyond pure theoretical interest, does the FCP-pair scheme possess any practical significance when similar inversion control can be accomplished with much longer pulses? To address this question, it is worthwhile to point out that the standard pulse-area approach only works on-resonance or near-resonance. This means that a TLS under study must be paired with a laser whose operating wavelength matches the transition wavelength of the TLS. However, in practice, such a requirement may not always be satisfied due to the availability of laser media, and this wavelength specificity in turn limits what kind of atomic systems a particular type of laser can serve. Meanwhile, a scheme based on FCP is able to tolerate a very large detuning as shown in our analysis ($\Delta \approx 0.089\omega_{ba}$ in the current case). This also implies that a single laser can potentially serve a wide range of atomic transitions. From these points of view, the FCP-pair scheme outlined above indeed offers a unique addition to the existing approaches of coherent control with experimental implications.

As an example, a hypothetical experimental scheme is conceived as follows. A free-run few-cycle ultrafast laser serves as the light source. There is no need for complicated CEP stabilization here because the final inversion depends only on the CEP difference between the two pulses. The laser output is split into two paths with a fixed path-length difference (e.g., 50 fs). A CEP tuning mechanism, such as a CaF_2 wedge pair, is introduced in the longer path, which allows the CEP of the trailing pulse to be precisely adjusted. The two paths then converge onto the two-level atomic sample to be controlled. An independent and weaker pulse can be introduced to probe the inversion state of the sample. It can also be used to calibrate the exact relation between w_f and φ_{CE2}. The pulse amplitudes in both paths can remain unchanged throughout the experiment. This not only simplifies the control scheme but also prevents any amplitude-induced inversion variation. A simple estimation shows that the field strength required in Fig. 5(a) is easily attainable with a 5-fs Ti:Sapphire oscillator of 100 mW average power and 80 MHz repetition rate. By adjusting φ_{CE2}, the inversion of the atomic system is expected to change following a regular sinusoidal relation as shown in Fig. 1(b).

It should be noted that coherent atom-field interactions involving femtosecond pulse sequences have been subjects of research in other contexts. For example, Scherer *et al.* used phase-locked sequences of femtosecond pulses to study time-resolved dynamics of isolated molecular systems [31] and wave packet interferometry [32,33]. Brinks *et al.* reported the observation and manipulation of vibrational wave-packet interference in individual molecules at ambient conditions [34]. The same group later demonstrated that quantum coherences in single organic molecules can be established, probed and controlled in highly disordered solid environments by applying femtosecond phase-locked double-pulse sequences [35]. More recently, Svidzinsky *et al.* showed that atomic coherence initiated by a leading pulse helps a trailing pulse generate Rabi oscillations in a TLS even when the latter pulse is a highly detuned adiabatic pulse [36].

The current research shares similar general ideas with these prior works but with a more specific emphasis on few-cycle pulses and CEP. Moreover, it must be clarified here that, although our findings identify CEP difference as the key factor determining the final inversion in the weak-field region, the effect should not be misunderstood as merely depending on the relative phase between the two pulses. The concept of CEP is crucial in the current context and the above reported effects cannot be produced by a pair of pulses much longer than the optical cycle, where CEP is no longer well-defined.

Finally, we would like to point out that all the results presented above are obtained under the relaxation-free approximation. We have, however, performed simulations with both T_1 and T_2

OSA CONTINUUM

considered. The results generally show a time-dependent reduction of the CEP sensitivity of the final inversion, which appears to be a straightforward extension of the relaxation-free results and provides little information fundamentally different. Therefore, these results are not presented here.

In conclusion, we have presented a numerical study on CEP-sensitive population inversion in a TLS induced by a FCP pair. Strong correlations are found between the final inversion and the CEPs of both pulses. Such inversion-CEP relations are modulated by peak Rabi frequencies (proportional to pulse amplitudes), creating distinctive weak-field and strong-field regions with markedly different characteristics. Carrier-wave Rabi flopping is identified as the key mechanism separating the two regions. Within the weak-field region, the inversion is found to only depend on the difference between the two CEPs. This is believed to be the result of coherence transfer executed by the TLS between the two pulses. The finding can potentially lead to a new scheme for coherent control based on FCP pairs. Its low power requirement offers a clear advantage over the single-pulse schemes, and its broadband nature results in improved wavelength flexibility when compared to the traditional method based on pulse area.

Funding

National Science Foundation (NSF) (ECCS-1254902).

Acknowledgment

The authors thank Dr. Michael Scalora of U.S. Army Aviation & Missile Research Development & Engineering Center (AMRDEC) for instructive discussions.

References

1. B. W. Shore, "Coherent manipulations of atoms using laser light," Acta Physica Slovaca **58**, 243–486 (2008).
2. R. Garcia-Fernandez, A. Ekers, L. P. Yatsenko, N. V. Vitanov, and K. Bergmann, "Control of population flow in coherently driven quantum ladders," Phys. Rev. Lett. **95**(4), 043001 (2005).
3. E. A. Shapiro, V. Milner, C. Menzel-Jones, and M. Shapiro, "Piecewise adiabatic passage with a series of femtosecond pulses," Phys. Rev. Lett. **99**(3), 033002 (2007).
4. E. A. Shapiro, V. Milner, and M. Shapiro, "Complete transfer of populations from a single state to a preselected superposition of states using piecewise adiabatic passage: Theory," Phys. Rev. A **79**(2), 023422 (2009).
5. S. Zhdanovich, E. A. Shapiro, J. W. Hepburn, M. Shapiro, and V. Milner, "Complete transfer of populations from a single state to a preselected superposition of states using piecewise adiabatic passage: Experiment," Phys. Rev. A **80**(6), 063405 (2009).
6. D. Feliinto, C. A. C. Bosco, L. H. Acioli, and S. S. Vianna, "Coherent accumulation in two-level atoms excited by a train of ultrashort pulses," Opt. Commun. **215**(1-3), 69–73 (2003).
7. D. Felinto, L. H. Acioli, and S. S. Vianna, "Accumulative effects in the coherence of three-level atoms excited by femtosecond-laser frequency combs," Phys. Rev. A **70**(4), 043403 (2004).
8. P. Kumar and A. K. Sarma, "Frequency-modulated few-cycle optical-pulse-train-induced controllable ultrafast coherent population oscillations in two-level atomic systems," Phys. Rev. A **87**(2), 025401 (2013).
9. J. H. Eberly, "Optical pulse and pulse-train propagation in a resonant medium," Phys. Rev. Lett. **22**(15), 760–762 (1969).
10. R. Teets, J. Eckstein, and T. W. Hansch, "Coherent two-photon excitation by multiple light pulses," Phys. Rev. Lett. **38**(14), 760–764 (1977).
11. J. Mlynek and W. Lange, "High-resolution coherence spectroscopy using pulse trains," Phys. Rev. A **24**(2), 1099–1102 (1981).
12. N. V. Vitanov and P. L. Knight, "Coherent excitation of a two-state system by a train of short pulses," Phys. Rev. A **52**(3), 2245–2261 (1995).
13. F. X. Kärtner, *Few-Cycle Laser Pulse Generation and its Applications* (Springer, 2004).
14. O. D. Mücke, T. Tritschler, M. Wegener, U. Morgner, and F. X. Kärtner, "Signatures of carrier-wave Rabi flopping in GaAs," Phys. Rev. Lett. **87**(5), 057401 (2001).
15. T. Brabec and F. Krausz, "Intense few-cycle laser fields: Frontiers of nonlinear optics," Rev. Mod. Phys. **72**(2), 545–591 (2000).
16. Y. Wu and X. Yang, "Strong-coupling theory of periodically driven two-level systems," Phys. Rev. Lett. **98**(1), 013601 (2007).

OSA CONTINUUM

17. A. A. Zabolotskii, "Integrable equations of a few cycle optical pulse propagation," Eur. Phys. J. Spec. Top. **173**(1), 193–222 (2009).
18. S. Hughes, "Breakdown of the area theorem: carrier-wave Rabi flopping of femtosecond optical pulses," Phys. Rev. Lett. **81**(16), 3363–3366 (1998).
19. J. Xiao, Z. Wang, and Z. Xu, "Area evolution of a few-cycle pulse laser in a two-level-atom medium," Phys. Rev. A **65**(3), 031402 (2002).
20. D. V. Novitsky, "Propagation of subcycle pulses in a two-level medium: Area-theorem breakdown and pulse shape," Phys. Rev. A **86**(6), 063835 (2012).
21. L. Allen and J. H. Eberly, *Optical Resonance and Two-Level Atoms* (Dover Publications, 1987).
22. Y. V. Rostovtsev, H. Eleuch, A. Svidzinsky, H. Li, V. Sautenkov, and M. O. Scully, "Excitation of atomic coherence using off-resonant strong laser pulses," Phys. Rev. A **79**(6), 063833 (2009).
23. P. K. Jha, H. Eleuch, and Y. V. Rostovtsev, "Coherent control of atomic excitation using off-resonant strong few-cycle pulses," Phys. Rev. A **82**(4), 045805 (2010).
24. G. G. Paulus, F. Grasbon, H. Walther, P. Villoresi, M. Nisoli, S. Stagira, E. Priori, and S. De Silvestri, "Absolute-phase phenomena in photoionization with few-cycle laser pulses," Nature **414**(6860), 182–184 (2001).
25. O. D. Mücke, T. Tritschler, M. Wegener, U. Morgner, F. X. Kärtner, G. Khitrova, and H. M. Gibbs, "Carrier-wave Rabi flopping: role of the carrier-envelope phase," Opt. Lett. **29**(18), 2160–2162 (2004).
26. C. Jirauschek, L. Duan, O. D. Mucke, F. X. Kärtner, M. Wegener, and U. Morgner, "Carrier-envelope phase-sensitive inversion in two-level systems," J. Opt. Soc. Am. B **22**(10), 2065–2075 (2005).
27. Y. Wu and X. Wang, "Carrier-envelope phase-dependent atomic coherence and quantum beats," Phys. Rev. A **76**(1), 013832 (2007).
28. W. Yang, X. Yang, and R. Lee, "Carrier-envelope-phase dependent coherence in double quantum wells," Opt. Express **17**(18), 15402–15407 (2009).
29. H. Li, V. A. Sautenkov, Y. V. Rostovtsev, M. M. Kash, P. M. Anisimov, G. R. Welch, and M. O. Scully, "Carrier-envelope phase effect on atomic excitation by few-cycle rf pulses," Phys. Rev. Lett. **104**(10), 103001 (2010).
30. E. W. L. Mandel, *Optical Coherence and Quantum Optics* (Cambridge University Press, 1995).
31. N. F. Scherer, A. J. Ruggiero, M. Du, and G. R. Fleming, "Time resolved dynamics of isolated molecular systems studied with phase-locked femtosecond pulse pairs," J. Chem. Phys. **93**(1), 856–857 (1990).
32. N. F. Scherer, R. J. Carlson, A. Matro, M. Du, A. J. Ruggiero, V. R. Rochin, J. A. Cina, G. R. Fleming, and S. A. Rice, "Fluorescence-detected wave packet interferometry: Time resolved molecular spectroscopy with sequences of femtosecond phase-locked pulses," J. Chem. Phys. **95**(3), 1487–1511 (1991).
33. N. F. Scherer, A. Matro, L. D. Ziegler, M. Du, R. J. Carlson, J. A. Cina, and G. R. Fleming, "Fluorescence-detected wave packet interferometry. II. Role of rotations and determination of the susceptibility," J. Chem. Phys. **96**(6), 4180–4194 (1992).
34. D. Brinks, F. D. Stefani, F. Kulzer, R. Hildner, T. H. Taminiau, Y. Avlasevich, K. Mullen, and N. F. van Hulst, "Visualizing and controlling vibrational wave packets of single molecules," Nature **465**(7300), 905–908 (2010).
35. R. Hildner, D. Brinks, and N. F. van Hulst, "Femtosecond coherence and quantum control of single molecules at room temperature," Nat. Phys. **7**(2), 172–177 (2011).
36. A. A. Svidzinsky, H. Eleuch, and M. O. Scully, "Rabi oscillations produced by adiabatic pulse due to initial atomic coherence," Opt. Lett. **42**(1), 65–68 (2017).